Catalysis Letters 30 (1995) 77–85

Structure of small Ni clusters on SiO_2

A. Jentys [a,b], D.H. Gay [b] and A.L. Rohl [b]

[a] *Institut für Physikalische Chemie, TU Wien, Getreidemarkt 9, A-1060 Vienna, Austria*

[b] *Davy-Faraday Laboratory, The Royal Institution of Great Britain, 21 Albemarle Street, London, W1X 4BS, UK*

Received 8 July 1994; accepted 2 November 1994

The geometry of small, silica supported Ni clusters has been studied using quantum mechanical cluster calculations and energy minimization techniques. A strong distortion from a spherical particle shape was found when the metal was in contact with the support. This resulted in a smaller average coordination number compared with isolated metal particles and in an increase of the interatomic distance for small particles.

Keywords: Ni/SiO_2; particle shape; clusters on surfaces

1. Introduction

For understanding the catalytic properties of supported metal catalysts, a detailed knowledge about size and shape of the metallic clusters is vital. Previous computational studies, which have been done on small metal clusters, have employed a variety of techniques, including geometrical considerations [1–3], the embedded atom method [4,5] and molecular dynamics methods [6–8]. However, only a few studies [1,9] have dealt with supported particles, while most of them considered only isolated metal clusters and neglected the crucial interaction with the support. But, the determination of the size of metal particles, as e.g. by EXAFS, relies strongly on an accurate knowledge of the relationship between the mean coordination number and the particle size. Especially for small clusters, deficiencies in the model for the particle geometry can cause large errors in the resulting particle size. Recently, Clausen et al. [6] reported that the particle size of silica supported Cu clusters, when calculated from EXAFS by using the relation from ref. [1], was smaller than when determined from XRD. In their work, the difference was explained with a non-Gaussian distribution of the distances within the particle and the authors developed a model for the particle shape based on molecular dynamics simulations [6,10].

In this work we studied the shape of small, silica supported Ni clusters. Consider-

ing this as a new application for atomistic modelling techniques, a reliable set of potential energy functions to describe the interaction between the atoms of the Ni particle and between the Ni particle and the silica surface had to be derived. To obtain these functions, we performed ab initio local density approximation calculations on cubes consisting of four Ni atoms and on a cluster representing a part of the silica surface together with a Ni atom. The parameters of the potential energy function were fitted to the binding energy as function of the geometry and used subsequently in atomistic simulations.

2. Methods

2.1. SURFACE SIMULATION TECHNIQUE

The atomistic simulation of the surface geometry was performed using the program MARVIN [11]. This program uses two-dimensional periodic boundary conditions with a two-dimensional Ewald summation [12,13] for calculating the total energy of a periodical, two-dimensional system.

The program divides the volume it is modelling into blocks, which are the basis of a two-dimensional repeat unit. Each block is further divided into two regions. In the first region, the positions of the atoms are allowed to relax explicitly to minimise the total energy, while in the second region, they are kept on fixed positions. The purpose of the second region is to reproduce the effects of the infinite crystal upon the ions at the surface and molecules or atoms above the surface. Therefore, the total energy calculated is the energy of the ions in the first region with the rest of the crystal. The effective temperature of this simulation is therefore 0 K. Note, that XAS experiments are commonly carried out at liquid nitrogen temperatures in order to minimize the thermal motion of the atoms.

In order to reduce the computational time needed, the minimization was carried out in three steps. First, the geometry of the Ni cluster was optimized. Then, the cluster was placed in close proximity to the silica surface, which was already in an energetically optimized geometry, and only the Ni cluster was allowed to relax. In the final step, the positions of the atoms of the Ni cluster and of the silica (in the surface region) were not restricted during the energy minimization.

2.2. THE QUANTUM MECHANICAL CLUSTER METHOD

The quantum mechanical cluster calculations, which were used for deriving the potentials, are based on local density functional equations (LDF), which were solved variationally and self-consistently [14,15]. In common with other LDF methods, the kinetic energy was calculated directly from the wave functions, while the Coulomb interactions were determined from the charge density. The many-electron exchange correlation term was calculated from the charge density as

derived by Barth and Hedin [16]. By using a double numeric basis set [15,17], which included additional double numeric core and higher angular momentum number polarization functions, negligible basis set superposition errors were guaranteed. The DMol code was employed in this study [18].

2.3. DETERMINATION OF THE INTERATOMIC POTENTIALS

The potentials, which were used in the atomistic simulations, are summarized in table 1.

The Ni–Ni potential was derived from a tetrahedral cluster consisting of four

Table 1
Potential parameters

Charges

Species	Charges
Si^{4+}	4.000
O^{2-}_{zeol} core	0.896
O^{2-}_{zeol} shell	−2.869
$O_{hydroxyl}$	−1.426
H	0.426
Ni	0.0

Buckingham potentials [a]

Species	A (eV)	ρ (Å^{-1})	C (eV Å^{-6})
Si^{4+}–O^{2-}	1283.90	0.3205	10.66
O^{2-}–O^{2-}	22764.47	0.1490	27.88
Ni–Ni	86502.0	0.1880	80.0
Ni–O	22830.0	0.2186	224.0

Morse potential [b]

	D_e (eV)	α (Å^{-1})	r_0 (Å)
$O_{hydroxyl}$–H	7.0525	2.1986	0.9485

Three body terms [c]

Species	K (eV rad^{-2})	θ_0
O–Si–O	2.09724	109.47

Shell model parameters

Species	Shell charge	k (eV Å^{-2})
O^{2-}_{zeol}	−2.87	74.9

[a] $E(r) = Ae^{-r/\rho} - Cr^{-6}$.
[b] $E(r) = D_e(1 - e^{-\alpha(r-r_0)})^2$.
[c] $E(\theta) = \frac{1}{2}K(\theta_0 - \theta)^2$ (for both O species).

nickel atoms. This cluster was distorted from its energetically favoured geometry and the binding energy was calculated as a function of the distance between the Ni atoms. The potential parameters were obtained by fitting the dependence of the binding energy as function of the geometry of the Ni_4 cluster. These parameters are in good agreement with those calculated by Shim et al. [19].

To determine the interatomic potential, which describes the interaction between the metal particle and the silica at the interface, a cluster representing a small unit of SiO_2 was used. A Ni atom was placed in close proximity to the cluster and the variation of the binding energy as a function of the distance between the silica fragment and the Ni atom was determined quantum mechanically. The geometry of the silica cluster together with the Ni atom is shown in fig. 1.

The potentials were derived from the quantum mechanically calculated energy hypersurface by a least-squares fit to the binding energy for each of the conformations examined. This procedure was carried out using a cluster version of the program GULP [20] and follows the methodology used by Gale et al. [21] to derive potentials for α-alumina.

The potentials used for the silica surface are the potentials that have been used successfully for many simulations of SiO_2 systems, such as quartz and various silicious zeolites [22–24]. These potentials have been extended to include a hydrogen oxygen potential for the hydroxyl termination of the silica surface.

The only interaction that has been neglected is the charge–image charge interaction between the silica substrate and the metallic nickel cluster. This neglects the metallic character of the larger clusters, and avoids the question of how many atoms it takes to make a metal. The effect of this energy on the cluster shape will be small since the charge–image charge interaction will only affect the silica surface and not the Ni atoms, because their charge is zero. Thus any perturbation of the Ni coordinates is a secondary effect.

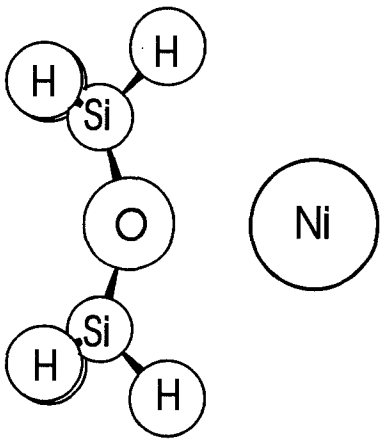

Fig. 1. Geometry of the Ni–SiO_2 cluster used for the determination of the Ni–O potentials.

Furthermore, since full ionic charges are used for the silica, which is a strongly covalent material, the magnitude for the charge–image charge interaction would be overstated. The spherical shape of the cluster will cause the image charges to be clustered in a small volume, reducing their effect.

3. Results and discussion

The geometries of isolated Ni particles and that of Ni clusters interacting with the (110) SiO_2 surface were calculated. We chose the (110) surface, because recent calculations showed that this surface is the most stable surface of SiO_2 [25].

The average coordination number for the first coordination shell of Ni, including all atoms at distances between 2 and 3 Å, is plotted in fig. 2 and the average distance between the Ni atoms in the first coordination shell in fig. 3. For comparison, the average coordination numbers of cuboctahedral clusters, obtained from Fritsche et al. [3], are included in fig. 2.

For perfect, cuboctahedral particles of 13 atoms an average coordination number for the first shell of 5.54 was reported [3]. For an isolated particle of the same size we obtained in our calculations 5.46, which is in good agreement with the reported number and suggests that the cuboctahedral geometry is preferred for small, isolated Ni particles. Note, that only particles with 13, 55, 147, etc. atoms can form perfect cuboctahedral clusters. The distance between the atoms of the isolated Ni particles was found not to depend on the size. A distance of 2.480 Å, slightly larger than the distance of bulk Ni (2.475 Å), was obtained for all particle sizes.

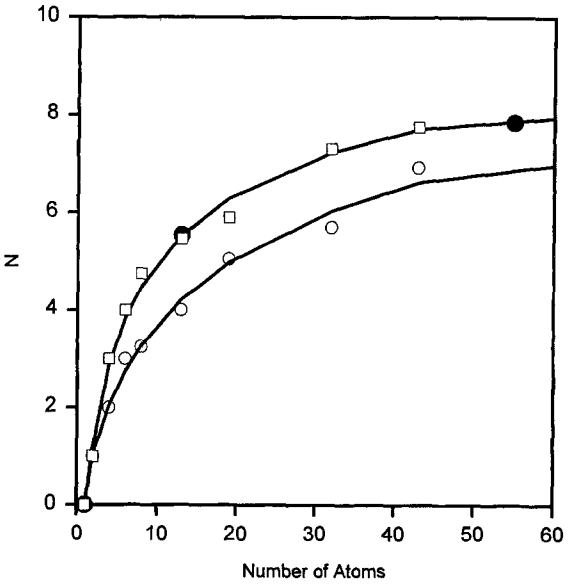

Fig. 2. Average coordination number of the first Ni shell as a function of the cluster size. (□) Isolated cluster, (●) cuboctahedral particle, (○) Ni/SiO_2.

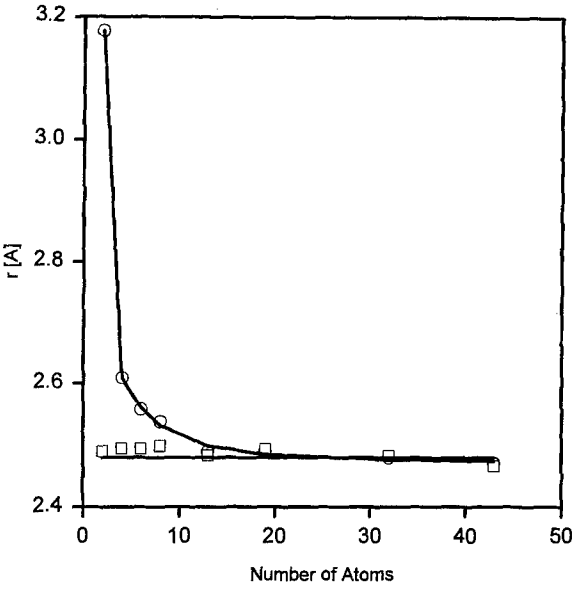

Fig. 3. Interatomic Ni–Ni distance as a function of the cluster size. (○) Ni/SiO_2, (□) isolated Ni cluster.

For Ni clusters in contact with the SiO_2 surface, we found their shape strongly affected. This was reflected in both, in the average coordination number and in the distance between the atoms. The average coordination number of Ni in the first coordination shell was significantly lower compared with isolated particles. The distance between the metal atoms was strongly enlarged for the cluster with two atoms and decreased with increasing cluster size. For clusters of up to eight atoms, the proximity of the SiO_2 surface caused the Ni atoms to penetrate into the surface of the support. For these cluster sizes, the minimization resulted in a structure where the metal atoms did not form a joined particle, but were arranged in a detached ensemble. This causes the distance between the Ni atoms to be much larger than in the isolated particles. The geometry of the Ni cluster consisting of eight Ni atoms on the SiO_2 surface is shown in fig. 4.

The formation of interconnected clusters started with a cluster size of 13 Ni atoms. For these clusters the distance between the atoms was close to the bulk value, but the shape was strongly distorted, causing the coordination number of the first shell to be below that for isolated clusters. The shape of a cluster consisting of 32 Ni atoms is shown in fig. 5.

4. Conclusions

The calculations presented, clearly show that the geometry of small, silica supported nickel clusters strongly depends on the interaction with the support. The dis-

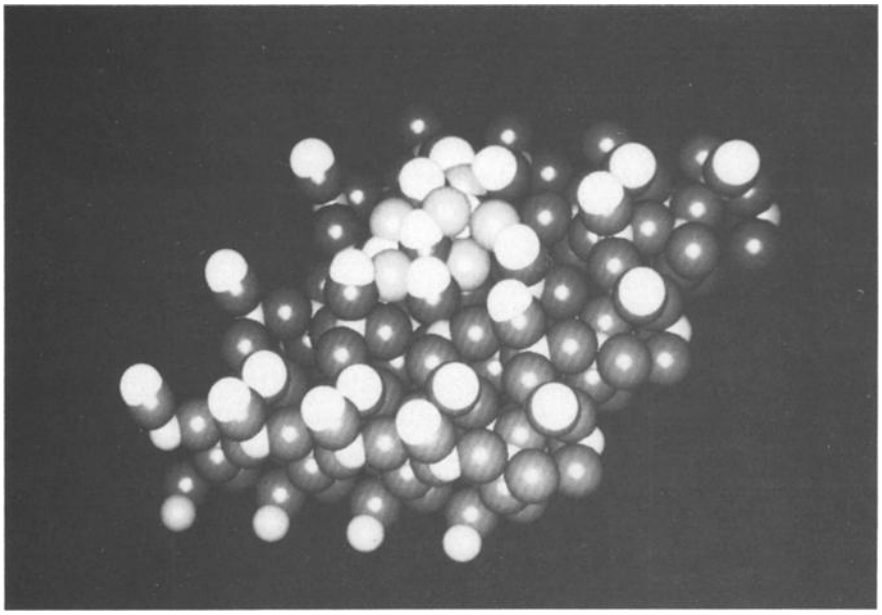

Fig. 4. Geometry of the eight-atom Ni cluster on the (110) surface of SiO_2.

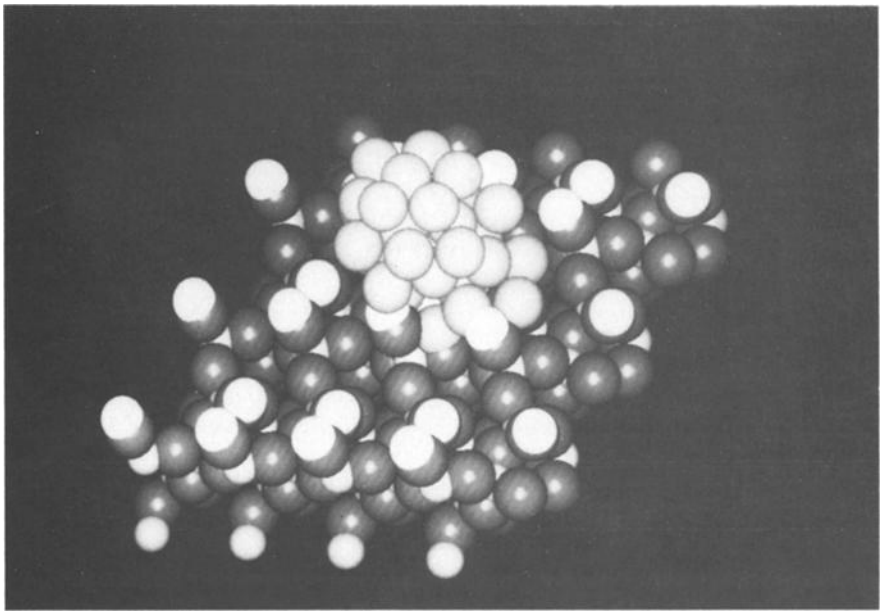

Fig. 5. Geometry of the 32-atom Ni cluster on the (110) surface of SiO_2.

tortion in the shape of the particle resulted in a significantly smaller average coordination number of the nearest neighbours compared to isolated clusters. For very small clusters the distance between the atoms is larger compared to the bulk, while for cluster sizes of 13 atoms and above the bulk value was observed. For the smaller clusters (2–8 Ni atoms) the interaction between the Ni atoms and the support caused the metal atoms to be spread across the surface and to be located between the terminal SiOH groups of the silica. With increasing particle size, the interaction between the metal atoms became more important, resulting in the formation of distorted, but dense packed metal clusters.

When the average coordination number is utilized to determine the particle size, our calculations clearly show that the interaction of the particle with the surface cannot be ignored. Otherwise, the calculated particle size would be significantly too small. On the basis of our calculations, we attribute this difference to the strong distortion from a quasi-spherical particle shape, caused by the contact of the metal with the surface of the support.

Acknowledgement

Financial support from the EC under the Science plan Grant SCI-0199, the Christian Doppler Laboratory for Heterogeneous Catalysis and Biosym Technologies are gratefully acknowledged.

References

[1] R.B. Greegor and F.W. Lytle, J. Catal. 63 (1980) 476.
[2] R.E. Benfield, J. Chem. Soc. Faraday Trans. 88 (1992) 1107.
[3] H.G. Fritsche and R.E. Benfield, Z. Phys. D 26S (1993) 15.
[4] A. Sachdev, R.I. Masel and J.B. Adams, J. Catal. 136 (1992) 320.
[5] A. Sachdev, R.I. Masel and J.B. Adams, Catal. Lett. 15 (1992) 57.
[6] B.S. Clausen, L. Gråbæk, H. Topsøe, L.B. Hansen, P. Stoltze, J.K. Nørskov and O.H. Nielsen, J. Catal. 141 (1993) 368.
[7] L.B. Hansen, P. Stoltze, K.J. Nørskov, B.S. Clausen and W. Niemann, Phys. Rev. Lett. 64 (26) (1990) 3155.
[8] J. Uppenbrink and D.J. Wales, J. Chem. Soc. Faraday Trans. 87 (2) (1991) 215.
[9] B.J. Kip, F.B.M. Duivenvoorden, D.C. Koningsberger and R. Prins, J. Catal. 105 (1987) 26.
[10] B.S. Clausen, H. Topsøe, L.B. Hansen, P. Stoltze and J.K. Nørskov, Jpn. J. Appl. Phys. 32 (1993) 95.
[11] D.H. Gay and A.L. Rohl, J. Chem. Soc. Faraday Trans., submitted.
[12] D.E. Parry, Surf. Sci. 49 (1975) 433.
[13] D.E. Parry, Surf. Sci. 54 (1976) 195.
[14] B.J. Delley, J. Chem. Phys. 92 (1990) 508.
[15] C. Sasa, J. Andzelm, B.C. Elkin, E. Wimmer, K.D. Dobbs and D.A. Dixon, J. Chem. Phys. 96 (1992) 6630.
[16] U. von Barth and L. Hedin, J. Phys. C 5 (1972) 1629.

[17] B. Delley, J. Chem. Phys. 92 (1990) 508.
[18] DMol version 2.1, BIOSYM Technologies, San Diego, USA (1991).
[19] I. Shim, J.P. Dahl and H. Johansen, Int. J. Quant. Chem. 15 (1979) 311.
[20] J.D. Gale, General Utility Lattice Program, Royal Institution of Great Britain, London (1993).
[21] J.D. Gale, C.R.A. Catlow and W.C. Mackrodt, Model. Simul. Mater. Sci. Eng. 1 (1992) 73.
[22] R.A. Jackson and C.R.A. Catlow, Mol. Sim. 1 (1988) 207.
[23] M. Sanders, M. Leslie and C.R.A. Catlow, J. Chem. Soc. Chem. Commun. (1984) 1271.
[24] S.D. Loades, S.W. Carr, D.H. Gay and A.L. Rohl, J. Chem. Soc. Chem. Commun. (1994) 1369.
[25] A.L. Rohl and D.H. Gay, to be published (1994).